Title
REACTION OF CHLORINE WITH LIQUID METALS I INDIUM

Authors
Balooch, M.
Siekhaus, W.J.
Olander, D.R.

Publication Date
1983-07-01

Lawrence Berkeley Laboratory

UNIVERSITY OF CALIFORNIA

Materials & Molecular Research Division

Submitted to the Journal of Physical Chemistry

REACTION OF CHLORINE WITH LIQUID METALS - I INDIUM

M. Balooch, W.J. Siekhaus, and D.R. Olander

July 1983

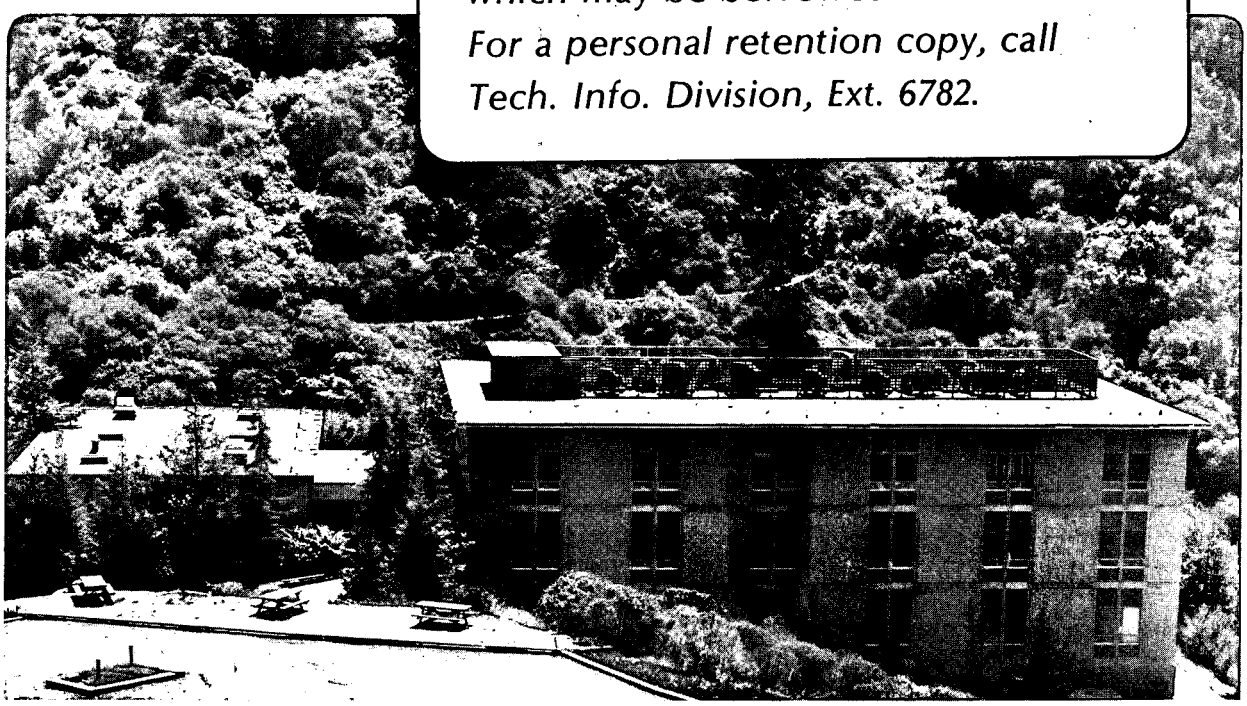

Prepared for the U.S. Department of Energy under Contract DE-AC03-76SF00098

DISCLAIMER

LBL-16357

REACTION OF CHLORINE WITH LIQUID METALS - I INDIUM

M. Balooch[+], W. J. Siekhaus[*] and D. R. Olander[+]

This work was supported by the Director, Office of Energy Research, Office of Basic Energy Sciences, Materials Sciences Division of the U. S. Department of Energy under contract #DE-AC03-76SF00098 and the U. S. Department of Energy under contract No. W-7405-Eng-48, and by the U. S. Army Research Office, Research Triangle Park, North Carolina under contract No. 15812-MS.

[+]Materials and Molecular Research Division of the Lawrence Berkeley Laboratory and the Department of Nuclear Engineering, University of California, Berkeley, California 94720

[*]Chemistry Division of the Lawrence Livermore National Laboratory

ABSTRACT

The reactions of molecular chlorine with liquid and solid indium surfaces were studied by modulated molecular beam-mass spectrometric methods in the temperature range 300-650 K and equivalent chlorine pressures of 4×10^{-6} - 4×10^{-4} Torr. In a separate chamber, the surface was monitored by AES as a function of temperature at an effective pressure of chlorine of 5×10^{-4} Torr. At high temperatures InCl was the only reaction product, while at low temperatures, $InCl_2$ desorption dominated. Near the melting point the behavior of the scattered Cl_2 signal suggested a drastic change in sticking probability, from that on a bare indium surface to one characterizing a chloride-covered surface. A reaction model based on dissociative adsorption of chlorine was developed from the molecular beam and AES data.

I. INTRODUCTION

During the past decade, understanding of gas-solid reactions has been greatly advanced by coupling of chemical kinetic techniques like modulated molecular beam mass spectrometry to surface analysis tools such as AES, LEED and ESCA(1). On the other hand, reactions of gases with liquids have recently come into technological prominence without comparable basic research attention. Such reactions occur in photoflash devices(2), propellants(3), steelmaking(4-6), high temperature flames(7), transpiration cooling(8), and passivation of liquid alloy surfaces(9). Performance estimates of yet-to-be-built devices such as the "wetted-wall" inertial confinement fusion reactor and the atomic vapor uranium isotope separator depend upon the kinetics of gas reactions with liquid metals.

For basic studies of gas-liquid reaction kinetics, the molecular beam or reactive scattering method with a halogen reactant gas and a low-melting point metal as the liquid reactant offers a number of advantages. The molecular beam method is well-suited to mechanistic studies because the beam modulation feature provides a direct measure of characteristic response times of the surface processes and because mass spectrometric detection permits identification of the chemical composition of the volatile reaction products. These and other desirable features, as well as limitations of the method, are reviewed in detail elsewhere(10 - 12). The unique feature of such a study is the ability to change drastically the nature of the surface on which the reaction occurs. Since the mechanisms and kinetics of gas-solid reactions are sensitive to the structure of the surface, the transformation of a solid surface to a liquid should be accompanied by profound changes in the reactivity of the metal

to chemical reactive gases.

Use of a halogen as the reactant gas has several desirable features. First, many halogen-metal reactions produce one or more volatile reaction products in easily accessible temperature ranges. Volatility of the product is of course a prerequisite for using in-situ mass spectrometric detection methods. Second, halogen-metal combinations are usually very reactive, which alleviates the sensitivity limitations to which the molecular beam technique is prone. Third, reactions of halogens with a variety of solid metals have been extensively studied for two decades using molecular beam or comparable low-pressure methods: fluorine reactions have been investigated on Ni(13), Ta(14) and other refractory metals(15 - 17); chlorine reactions have been studied on Ta(18), Fe(19), Ni(20), and Si and Ge(21); molecular beam studies of the heavier halogens with metals include Ni/Br_2(22) and Zr/I_2(23).

It would be desirable to study halogen-liquid phase reaction kinetics for the same systems that have already been the subject of molecular beam studies as solids. However, in reviewing the above list of metals used in such experiments, it is found that most have melting points which are too high to be of use experimentally in a molecular beam experiment. Consequently, lower-melting metals must be chosen, with the additional restriction that the vapor pressures over the liquid be sufficiently low so that loss by vacuum vaporization is not significant. These conditions are satisfied by the metals shown in Table 1. Indium is the metal investigated for this paper. The remaining three metals will be treated in subsequent parts of this series. In all cases, reaction on both the solid and liquid phases of the metal were studied. In some cases, however, the solid was so unreactive even at temperatures near the melting point

that only data on the reaction of the liquid phase were of quantitative value.

The apparatus, which is a slightly modified version of one described previously(14), is shown in Fig. 1. It consists of three differentially-pumped vacuum chambers separated by beam-forming orifices. The incident reactant beam is generated by effusion from the quartz source tubes which has a hole in the end. The tube contains chlorine gas at several Torr pressure, which is sufficiently low that the flow from the hole is effusive. A rotating toothed disk imparts a periodicity of 2 to 1000 Hz to this flux. The modulation frequency is detected by an optical switch for transmission to the phase-sensitive detection electronics. A 1 mm diameter collimator in the vacuum wall shapes this modulated flow into a thin pulsed beam of molecules which is $\sim$3 mm diameter as it strikes the solid or liquid metal surface (the target) held in the target chamber. The intensity of the incident molecular beam of chlorine during the "on" portion of the chopping cycle (I_o) can be calculated from the gas pressure in the source, the conductance of the hole in the end of the tube and the 4-cm source-to-target distance. This quantity can be converted to an equivalent reactant gas pressure by using the standard gas kinetic theory formulas, which yields:

$$P_{Cl_2} = \sqrt{\frac{71\ T_{beam}}{3.51 \times 10^{22}}}\ I_o = 4.2 \times 10^{-21}\ I_o \qquad \text{(Torr)}$$

Because of pumping limitations in the source chamber, the maximum achievable incident beam intensity is $\sim 10^{17}$ molecules/cm-s, or by the above formula, an equivalent chlorine pressure of $\sim 4 \times 10^{-4}$ Torr. The source tube is not heated, so the incident beam temperature is 300 K.

The target metal is held in a shallow molybdenum crucible heated by radiation. The metal is cycled through the melting point during the course of gathering data, so the structure of the solid surface is polycrystalline.

The cleanliness of the liquid surface is maintained by reaction with chlorine, which removes surface layers at greater rates than impurities can deposit from the vacuum system. The surface temperature is measured by an infrared pyrometer which is calibrated on the melting point of the metal prior to the experiment. The target chamber is pumped by a well-trapped oil diffusion pump to a typical base pressure of 5×10^{-9} Torr.

Portions of the scattered chlorine and desorbed reaction products are detected by a quadrupole mass spectrometer mounted in the detection chamber, which communicates with the reaction chamber via a 1mm-diameter orifice. This collimator serves to admit the gas mixtures emanating from the target into the ionizer of the mass spectrometer as a well-defined beam. Collimation is necessary to prevent collisions of the molecules produced at the target with the structure of the mass spectrometer, which could result in spurious reaction or at least undesirable multiple scattering events. The mass spectrometer ionizer is 4 cm distant and in direct line-of-sight view of the beam spot on the target. For maximum sensitivity, ionization is conducted with 70V electrons. The operating pressure of the ion-pumped, all-metal detection chamber is 10^{-10} Torr.

The output from the mass spectrometer is processed by a lock-in amplifier with a two-phase accessory to yield the first Fourier components. The apparent reaction probability ε (the ratio of the amplitudes of the product and reactant signals, corrected for ionization efficiencies of the mass spectrometer) and the phase lag ϕ, which is the difference between the product and the reactant phase angles, are obtained from the information provided by the lock-in amplifier(10). A complete set of molecular beam data consists of measurements of ε and ϕ as functions of the

three controllable experimental variables, which are the surface temperature (T), the modulation frequency of the molecular beam (f) and the beam intensity at the surface (I_o). In conducting experiments, one variable is changed while the other two are kept constant.

In a separate apparatus, (Fig. 2), the surface composition is analyzed by an Auger electron spectrometer while the target is subjected to a chlorine beam of the same intensity as in the modulated molecular beam test. The chlorine beam is provided by a doser and the beam intensity is calculated from the upstream pressure reading and the conductance of the doser. The system is pumped with a well-trapped diffusion pump. A typical base pressure is $\sim 10^{-8}$ Torr.

III. DATA ANALYSIS

The data from a molecular beam experiment, processed to the form of the apparent reaction probability ε and the reaction phase lag ϕ as functions of T, f and I_o, can only be understood in terms of a model of the reactions occuring on the surface. Reaction models must be developed quantitatively to produce theoretical ε and ϕ predictions as functions of the same experimental variables. These predictions are compared with the ensemble of the molecular beam data using an appropriate optimization computer code as well as with the AES surface composition results where these are available. Selection of the best reaction model is determined by several criteria. First, the model should fit the data better than its competitors. Second, the model should contain the fewest possible adjustable parameters. Third, the preexponential factors and activation energies of the rate constants contained in the model should be within

ranges suggested by theory and by previous experience.

Although model selection is a tedious procedure, it can be expedited by recognizing distinctive features of the data which signal the presence of particular steps in the surface process, or which directly yield a numerical value of a parameter. For example, if the temperature is sufficiently high, all kinetic processes on the surface become fast compared to the characteristic modulation period of a few milliseconds. In this limit, the phase lag is near zero and the apparent reaction probability is temperature-independent. The latter, therefore, is equal to the sticking probability of Cl_2 on the surface. Examples of "signatures" of particular elementary steps are (10,11): a 45° phase lag independent of all experimental variables, which indicates control of the surface processes by diffusion of one of the intermediates in the bulk solid (or liquid); a maximum in the variation of the phase lag with modulation frequency, which is a certain indicator of a branched process in the mechanism; any variation of ε and ϕ with incident beam intensity, which is a sign of a nonlinear step in the mechanism.

Quantitative implementation of a mechanistic model begins by writing balances on all reaction intermediates present on the surface or in the bulk near the surface. Invariably, dissociative chemisorption of Cl_2 from the incident beam is the first step in any mechanism. The balance on chlorine adatoms is of the general form:

$$\dot{n} = R_{ads} - R_{rxn} - R_{diff} \qquad (1)$$

where $\dot{n}$ is the time derivative of the surface chlorine atom concentration and R_{ads} is the rate of supply of this species from the incident Cl_2 beam.

Modulation of this supply term is described by the gating function g(t) of the beam chopper, which is very close to a square wave of period f Hz. Removal terms in the surface chlorine balance include surface reactions, generically labeled R_{rxn}, and possibly diffusion into the bulk substrate at a rate given by R_{diff}. If the model contains other surface intermediates, balance equations are needed for each of these as well. For example, if the surface reaction in Eq(1) creates the product molecule as an adsorbed species which then desorbs to produce the gaseous species detected by the mass spectrometer, the appropriate balance equation is:

$$\dot{m} = R_{rxn} - R_{des} \qquad (2)$$

where m is the concentration of the adsorbed product molecule, and the last term is its rate of desorption.

The model supplies explicit expressions for the rates on the right hand sides of Eqs(1) and (2) in terms of surface concentrations n and m, the incident beam intensity, sticking probabilities, rate constants, diffusion coefficients, etc. The mathematical treatment of the time-dependent surface balance equations to produce theoretical apparent reaction probabilities has been described in detail elsewhere(11, 24-27). Basically, the periodic variation of the incident molecular beam and the responses of the concentrations of all intermediates are represented by steady state components plus the first Fourier components (fundamental modes). Solutions of the surface mass balances (and a bulk diffusion equation, if needed) for the coefficients of these truncated Fourier expansions are obtained. The product desorption rate possesses both amplitude and phase because it is a cyclically-varying quantity with the same frequency as g(t) but of a different shape. The reaction product vector from

which ε and ϕ are determined is defined as the ratio of the fundamental modes of the product desorption rate to that of the reactant impingement rate. In this paper and those that follow in this series, the mathematical details of the conversion of a reaction model to predicted ε and ϕ as functions of T, f and I_o will not be given. Only the surface mass balances, which contain the essential physical and chemical features of the mechanism, will be presented.

IV. RESULTS

Above the melting point of the metal, the only indium-containing ions observed in the mass spectrometer were $InCl^+$ and In^+. The ratio of the $InCl^+$ and In^+ signals was $\sim$ 0.25 at all surface temperatures, and both signals had the same phase angle. The In^+ signal is clearly a fragment of dissociative ionization of InCl or a higher chloride. However, no parent ion of any higher indium-chloride could be detected at any ionizing electron energy.

During reaction with solid indium, $InCl^+$ was the predominant ion observed, although the production rate was an order of magnitude smaller than in reaction with the liquid metal. By reducing the energy of the ionizing electrons in the mass spectrometer, a small amount of $InCl_2^+$ (estimated to be $\sim$ 5%) was observed. However, because of the very low mass spectrometer sensitivity at low electron energies, both the $InCl^+$ and $InCl_2^+$ signals were near the noise level. Their phase angles could not be accurately determined.

The reaction probabilities reported below were computed by summing all indium-containing signals and dividing by the sum of the Cl_2^+ signal and one-half of the Cl signal. The latter arises mainly

from cracking of Cl_2 in the mass spectrometer ionizer. Signal ratios were converted to flux ratios using ionization cross section ratios obtained from Ref. 28 and the other instrumental efficiency factors and transit time effects discussed in Ref. 10. Since InCl is the predominant product, the maximum value at the reaction probability is two.

Figures 3 and 4 show the apparent reaction probability and phase lag as functions of temperature at the maximum Cl_2 incident beam intensity and for three modulation frequencies. There appears to be a discontinuous change in ε at the melting point (Fig. 3) but the phase lag, although dropping sharply prior to melting, appears to be a continuous function of temperature through the melting point (Fig. 4). No hystereis behavior in either ε or ϕ was observed during temperature cycling through the melting point.

The effect of beam intensity variation on ε and ϕ are shown in Fig. 5 for constant chopping frequency and for two temperatures, one just below and the other above the melting point. The lack of variation of ε and ϕ with beam intensity above the melting point suggests that the reaction is linear for the liquid phase. On the other hand, a slight nonlinearity is observed for the solid phase.

The frequency dependence of the apparent reaction probability and phase lag are shown in Figs. 6 and 7, again for four different temperatures covering both liquid and solid phases. At 598 K, the surface chemical process is fast with respect to the time scale of primary beam modulation so that the apparent reaction probability does not change appreciably with frequency and the phase lag is nearly zero.

The circles in Fig. 8 represent the ratio of the scattered chlorine signal at temperature T (designated by Cl_2^T on the plot) to the same

quantity when the target is unheated (Cl_2^R). A decrease in the output signal with increasing surface temperature can occur even if the scattered chlorine flux is constant because the mass spectrometer is a density-sensitive detector. Its output signal is proportional to the number density of molecules in the ionizer. This quantity can decrease at constant flux if the mean speed of the molecules increases due to heating of the unreacted Cl_2 beam by thermal accommodation of the incident molecules with the solid or liquid surface. The mean speed is inversely proportional to the square root of the temperature of the reflected molecules. The observation from Fig. 8 that the ratio Cl_2^T/Cl_2^R remains constant at unity between 300 K and the melting point of 429 K indicates that thermal accommodation of Cl_2 on the solid indium surface is poor. Had the thermal accommodation coefficient been unity, a decrease from unity to $(300/429)^{\frac{1}{2}} = 0.84$ would have been expected. The constancy of the scattered chlorine signal also indicates that very little reaction with the metal occurred. Between the melting point and $\sim$ 600 K, the reflected chlorine signal decreases by 8%. This reduction can be due to either to better thermal accommodation of the reflected chlorine molecules on the liquid surface than on the solid or to consumption of chlorine by reaction to form indium chloride. The latter explanation appears to be the more reasonable, because the chlorine deficiency of $\sim$ 8% at high temperature seen in Fig. 8 is consistent with the $\sim$ 10% reaction probability shown in Fig. 3 for the same temperature range.

Figure 9 shows the AES analysis of the surface chlorine concentration as a function of temperature at a beam intensity (delivered by the doser shown in Fig. 2) comparable to that used in the molecular beam experiments.

The Auger signal for chlorine was independent of temperature up to 400 K. This behavior was assumed to indicate complete coverage of the solid surface by chlorine and the AES signals at higher temperatures were normalized by the low temperature signal. Chlorine depletion of the surface when indium is liquid is evident from Fig. 9. However, the Cl/In ratio of the surface could not be quantitatively determined by AES.

V. DISCUSSION

The first requirement of a reaction model is specification of the reaction products. For the liquid metal reactant, the mass spectrometer signals unambiguously indicated InCl to be the only volatile reaction product. However, the product distribution for the solid metal reactant is not as straightforward. Here, the mass spectrometer detected primarily $InCl^+$, with a trace of $InCl_2^+$. Metal halides have a well-known propensity for extensive fragmentation by electron impact, especially at energies around the 70 V used in the present experiments; it is not uncommon to find no parent ions at all(29). Unfortunately, the fragmentation patterns of $InCl_2$ and $InCl_3$ are not available, but it is possible that these species made up part of the volatile products. Qualitatively, the mass spectrometer observations indicate that the chlorine-to-indium ratio of the product was lower for reaction of the liquid metal than for reaction with the solid phase. For reaction modeling purposes, it is assumed that the sole products of the reaction are the mono- and dichlorides. To represent the mass spectrometer observations, the model is constrained to produce much less of the latter when the metal is liquid than when it is solid.

The AES results in Fig. 9 indicate the formation at low temperature of a chlorine-saturated surface of undetermined stoichiometry on the solid metal. However, a few tens of degrees below the melting point, the chlorine signal begins to decrease, and by 500 K, 80% of the initial chlorine has disappeared from the surface. In the reaction model, the chlorine-saturated state of the surface just below $\sim$ 400 K is assumed to reflect monolayer coverage by InCl. Reduction in the chlorine signal at higher temperatures is attributed to breakup of this layer into islands of InCl on a bare metal surface.

The general lack of interaction of the Cl_2 beam with the fully-covered surface is suggested by the low reaction probability(Fig. 3) and the constant reflected chlorine signal(Fig. 8) at temperatures below 400 K. However, a small extent of reaction is observed on the solid metal. This can be attributed to minor adsorption of Cl_2 on the InCl layer followed by reaction to produce the dichloride.

When significant bare surface exposure occurs at approximately the melting point of indium, the reaction begins in ernest. This behavior suggests much more effective adsorption of chlorine by the bare metal than by the covered surface, in conjunction with more rapid production and evaporation of the InCl product due to the elevated temperatures.

The model qualitatively outlined above can be expressed by the following reactions:

$$Cl_2(g) \xrightarrow{\eta_1(1-\theta)} Cl(\text{ads on In}) \qquad (3)$$

$$Cl_2(g) \xrightarrow{\eta_2\theta} Cl(\text{ads on InCl}) \qquad (4)$$

where η_1 is the dissociative adsorption probability of molecular chlorine on the bare indium surface and η_2 is the comparable sticking probability on the InCl-covered portion of the surface. The probability of Cl_2 chemisorption on a unit area of surface is also proportional to the fraction of the surface in each state, as determined by the InCl coverage (θ).

InCl is produced by surface reaction of adsorbed chlorine and indium:

$$Cl(\text{ads on In}) + In \xrightarrow{k_1} InCl \qquad (5)$$

for which the rate constant is designated by k_1. Desorption of InCl is expressed by:

$$InCl \xrightarrow{k_d} InCl(g) \qquad (6)$$

Finally, chlorine adsorbed on the covered portion of the surface can react with this surface to produce $InCl_2$:

$$Cl(\text{ads on InCl}) + InCl \xrightarrow{k_2} InCl_2(g) \qquad (7)$$

for which the rate constant is k_2.

The concentration of chlorine adatoms on the bare and covered portions of the surface are denoted by n_1 and n_2, respectively. The surface balance on the total chlorine adatom population is:

$$\frac{d}{dt}[n_1(1-\theta) + n_2\theta] = 2I_o g(t)[\eta_1(1-\theta) + \eta_2\theta] - k_1 n_1(1-\theta) - k_2 n_2\theta \qquad (8)$$

The effective sticking probability of Cl_2 on the surface, which is the bracketed quantity in the first term on the right hand side, depends on InCl coverage and hence on temperature. However, the sticking probabilities for each surface, η_1 and η_2, are assumed to be temperature independent.

The total chlorine adatom balance needs to be supplemented by a relationship between the two subpopulations. The simplest connection is equilibrium partitioning with a distribution coefficient H:

$$n_2 = Hn_1 \tag{9}$$

The balance on the InCl surface species includes production by the reaction of chlorine with the bare metal and removal by desorption and by dichloride formation:

$$N_s \frac{d\theta}{dt} = k_1 n_1 (1-\theta) - k_2 n_2 \theta - k_d N_s \theta \tag{10}$$

where N_s is the surface density of sites.

Following the method outlined in Section III, these equations are solved by the Fourier expansion method and the reaction product vector is determined from the fundamental mode solutions of the InCl desorption rate and the $InCl_2$ production rate. The model parameters are chosen to provide the best fit to the molecular beam data, a process which produces the curves shown in Figs. 3 - 7. The sticking probabilities so determined are 0.08 and 1.5×10^{-3} for the bare and covered surfaces, respectively. The rate constants for the surface processes(with units of s^{-1}) are:

$$k_1 = 3 \times 10^{9} \, e^{-13/RT}$$

$$k_2 = 1 \times 10^{10} \, e^{-14/RT}$$

$$k_d = 3 \times 10^{14} \, e^{-28/RT}$$

where the activation energies are in kcal/mole and R is the gas constant. The other parameters used in the data fitting process are $N_s = 3 \times 10^{14}$ cm^{-2} and H = 0.1. The activation energy of the distribution coefficient H was less than a few kcal/mole.

The curve passing through the data points in Fig. 8 is one minus the effective sticking probability, which is the bracketed quantity in the first term on the right hand side of Eq(8). Because the model contains no provisions for reemission of either Cl_2 or Cl from the surface-adsorbed chlorine (which is consistent with past experience with halogen-metal reactions, see Refs. 13 - 23), chlorine which chemisorbs on the surface is removed from the scattered reactant flux detected by the mass spectrometer. The good accord between the observed reduction of scattered signal with increasing temperature and the model prediction in essence simply closes the mass balance on chlorine at the surface.

A more stringent test of the reaction model and the numerical values of its constituent rate constants is the ability to reproduce the AES data in Fig. 9. The model contains three forms of surface chlorine, the adatom populations with concentrations n_1 and n_2 and the chlorine contained in the InCl-covered part of the surface, with concentration $N_s\theta$. According to the model, the latter is by far the largest contributor to the total chlorine content of the surface, so that the data points in Fig. 9 should correspond to the steady state coverage of InCl on the reacting surface. This quantity can be computed for the steady Cl_2 beam used in the AES tests by setting the left hand sides of Eqs(8) and (10) equal to zero, replacing g(t) by unity in the adsorption term, and solving the resulting algebraic equations for the coverage θ. The results of this procedure using the rate constants given above, are shown as the curve in Fig. 9. The satisfactory agreement with the AES data constitutes independent verification of the model, which was developed entirely from the molecular beam data.

VI CONCLUSIONS

Data from modulated molecular beam experiments are interpreted in terms of a reaction mechanism involving chlorine adsorption and reaction on bare metal and InCl-covered portions of the surface. Sticking of Cl_2 occurs more readily on the former surface than on the latter, so that the effective sticking probability increases rapidly over the temperature range in which the surface becomes uncovered. The kinetics are also affected by slow desorption of the predominant InCl product.

The rate constants of the reaction change very rapidly at the melting point of indium, although not discontinuously. The AES data show loss of surface chlorine well below the melting point. The model deduced from the molecular beam data also satisfactorily predict the AES response of the surface to temperature.

ACKNOWLEDGEMENT

This work was supported by the Director, Office of Energy Research Office of Basic Energy Sciences, Materials Sciences Division of the U. S. Department of Energy under contract #DE-AC03-76SF00098 and the U. S. Department of Energy under contract No. W-7405-Eng-48, and by the U. S. Army Research Office, Research Triangle Park, North Carolina under contract No. 15812-MS.

REFERENCES

1) M. J. Cardillo, Ann. Rev. Phys. Chem. 32, 331 (1981).

2) T. H. Rantenberg, Jr. and P. D. Johnson, J. Opt. Soc. Amer. 50, 602 (1960).

3) H. Cheung and N.S. Cohen, AIAA J. 3, 250 (1965).

4) R. Baher, J. Iron Steel Inst. 205, 637 (1967).

5) L. A. Baher and R. G. Ward, J. Iron Steel Inst. 205, 714 (1967).

6) A. Hamielec, W. K. Lu and A. McLean, Can. Met. Quart. 1,27 (1968).

7) L. S. Nelson, H. S. Levine, D. E. Rosner and S. C. Kurzius, High Temp. Sci. 2, 343 (1970).

8) F. F. Muir, K. J. Tourya and R. Eichhorn, Sandia Lab. Report SC-DR-68-839 (1969).

9) C. G. Glen and F. D. Richardson, Proc. Int. Conf. on Heterogeneous Kinetics at Elevated Temperatures, Plenum Press, New York (1970).

10) R. H. Jones, D. R. Olander, W. H. Siekhaus and J. A. Schwarz, J. Vacuum Sci. Technol. 9, 1429 (1972).

11) J. A. Schwarz and R. J. Madix, Surf. Sci. 46,317 (1974).

12) D. R. Olander, J. Colloid and Interface Sci., 58, 169 (1977).

13) J. D. McKinley, J. Chem. Phys. 45, 1960 (1966).

14) A. J. Machiels and D. R. Olander, Surface Sci. 65, 325 (1977).

15) P. C. Nordine, J. Electrochem. Soc. 125, 498 (1978).

16) J. L. Philippart, J. Y. Caradec, B. Weber and A. Cassuto, J. Electrochem. Soc. 125, 162 (1978).

17) D. E. Rosner and H. D. Allendorf, J. Phys. Chem. 75, 308 (1971).

18) B. Weber, J. L. Philippart and A. Cassuto, Surface Sci. 52, 311 (1975).

19) M. Balooch, W. Siekhaus and D. R. Olander, Trans. Farad. Soc., to be published.

20) J. D. McKinley, J. Chem. Phys. 40, 120 (1964).

21) R. J. Madix and J. A. Schwarz, Surface Sci. 24, 264 (1971).

22) J. D. McKinley, J. Chem. Phys. 40, 576 (1964).

23) M. Balooch and D. R. Olander, J. Electrochem Soc. 130, 152 (1983).

24) H. C. Chang and W. H. Weinberg, Surf. Sci. 72, 617 (1978).

25) J. A. Schwarz and R. J. Madix, J. Catal. 12, 140 (1968).

26) H. C. Chang and W. H. Weinberg, Surf. Sci, 65, 153 (1977).

27) A. Ullman and D. R. Olander, Inter. J. Chem. Kinetics, Vol. VIII, 625 (1976).

28) J. B. Mann in "Recent Developements in Mass Spectroscopy," K. Ogata and T. Hayakawa, Editors, P. 814, University Park Press, Baltimore (1970).

29) D. L. Hildenbrand, private communication.

Table I. Vapor Pressures of Low-Melting-Point Liquid Metals

	Metal	Melting Point (K)	TEMPERATURES (K) at the indicated vapor pressure (Torr)	
			10^{-6}	10^{-8}
I	In	429	877	770
II	Pb	600	705	617
III	Bi	544	672	590
IV	Sn	505	1070	937

Figure Captions

1. Modulated molecular beam apparatus for investigation of the reactions of chlorine with liquid metals.
2. Vacuum chamber for surface examination by Auger electron spectroscopy during reaction with chlorine.
3. Temperature dependence of the apparent reaction probability.
4. Effect of temperature on the phase lag.
5. Effect of incident chlorine beam intensity on the components of the reaction product vector at temperatures above and below the melting point of indium.
6. Modulation frequency dependence of the apparent reaction probability.
7. Modulation frequency dependence of the phase lag.
8. Temperature dependence of the scattered chlorine signal; beam intensity = 1.1×10^{17} molecules/cm^2-s, modulation frequency = 20 Hz. The curve is the model prediction of one minus the effective sticking probability of Cl_2 on the surface.
9. Normalized AES signal from an indium surface exposed to a Cl_2 beam. The data are normalized to the signal at room temperature. The curve is the prediction of the reaction model based on the molecular beam data.

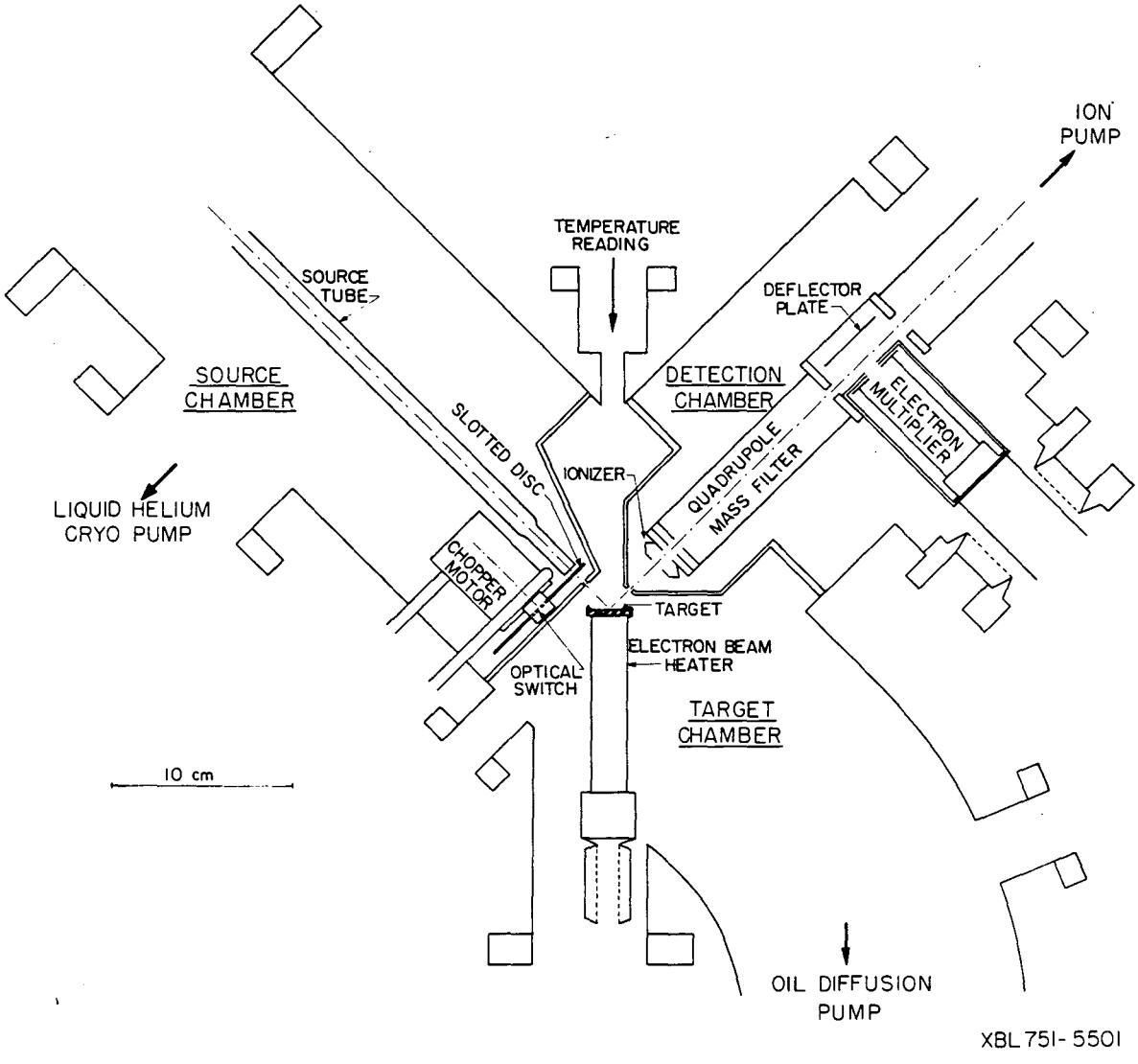
ION PUMP
TEMPERATURE READING
SOURCE TUBE
DEFLECTOR PLATE
SOURCE CHAMBER
DETECTION CHAMBER
ELECTRON MULTIPLIER
SLOTTED DISC
IONIZER
QUADRUPOLE MASS FILTER
LIQUID HELIUM CRYO PUMP
CHOPPER MOTOR
TARGET
ELECTRON BEAM HEATER
OPTICAL SWITCH
TARGET CHAMBER
10 cm
OIL DIFFUSION PUMP
XBL 751-5501

Fig. 1

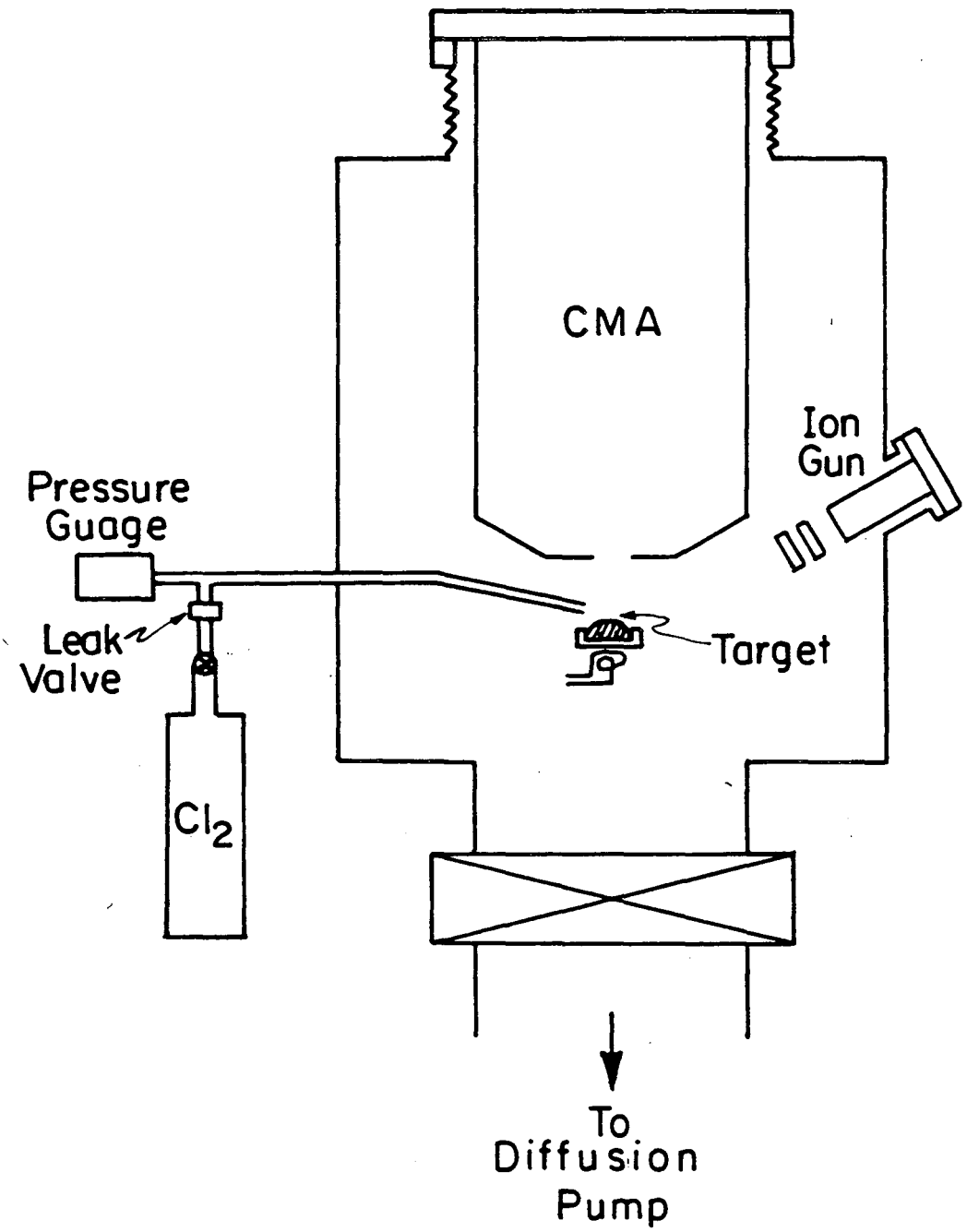
CMA
Ion
Gun
Pressure
Guage
Leak
Valve
Target
Cl_2
To
Diffusion
Pump
XBL 831-5169

Fig. 2

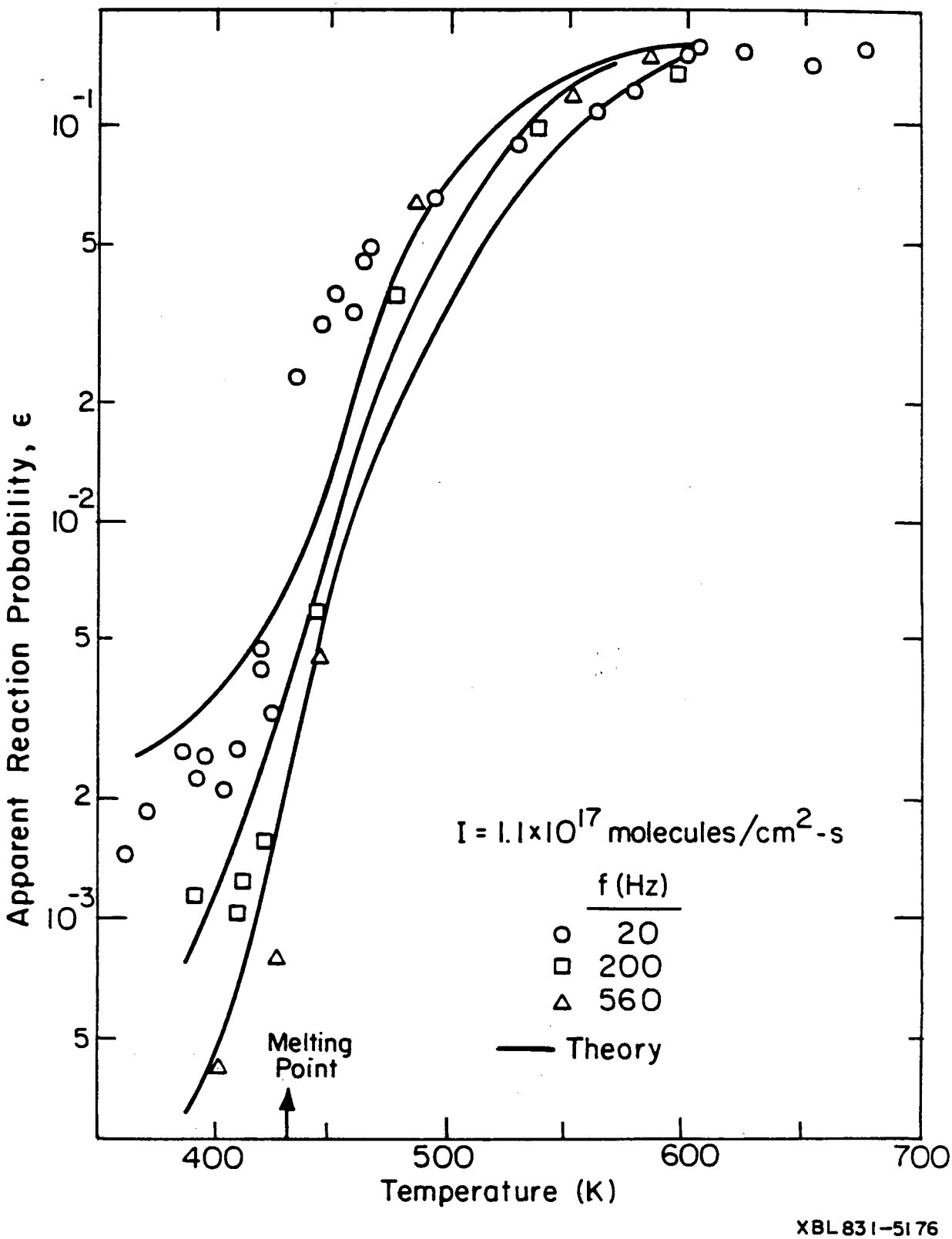
Apparent Reaction Probability, ε
10^-1
5
2
10^-2
5
2
10^-3
5
400
500
600
700
Temperature (K)
I = 1.1×10^17 molecules/cm^2-s
f (Hz)
20
200
560
Theory
Melting Point
XBL831-5176

Fig. 3

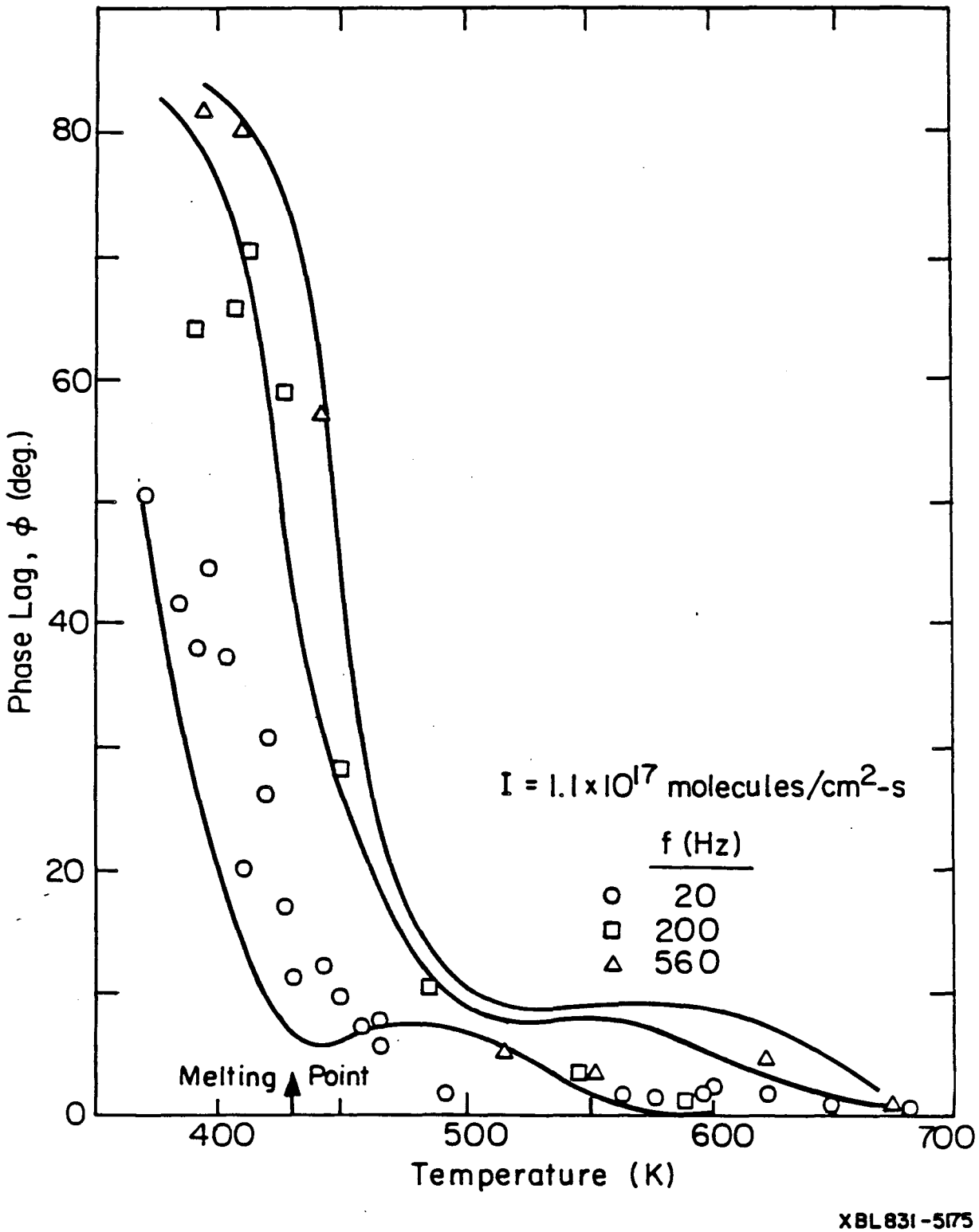
80
60
40
20
0
Phase Lag, ϕ (deg.)
400
500
600
700
Temperature (K)
I = 1.1 x 10^17 molecules/cm^2-s
f (Hz)
20
200
560
Melting Point
XBL831-5175

Fig. 4

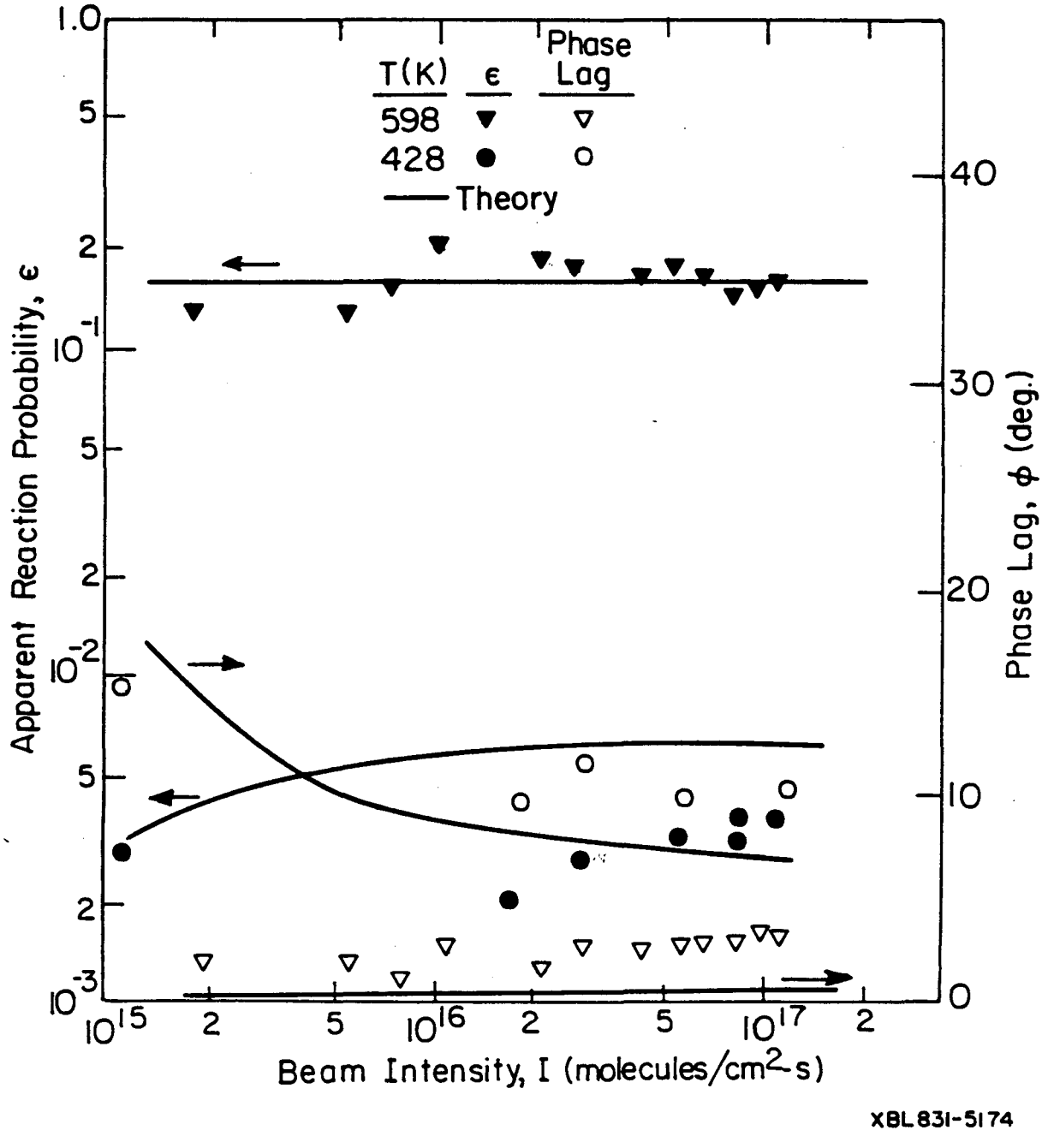
T(K)
ε
Phase Lag
598
428
Theory
Apparent Reaction Probability, ε
Phase Lag, φ (deg.)
Beam Intensity, I (molecules/cm²-s)
XBL831-5174

Fig. 5

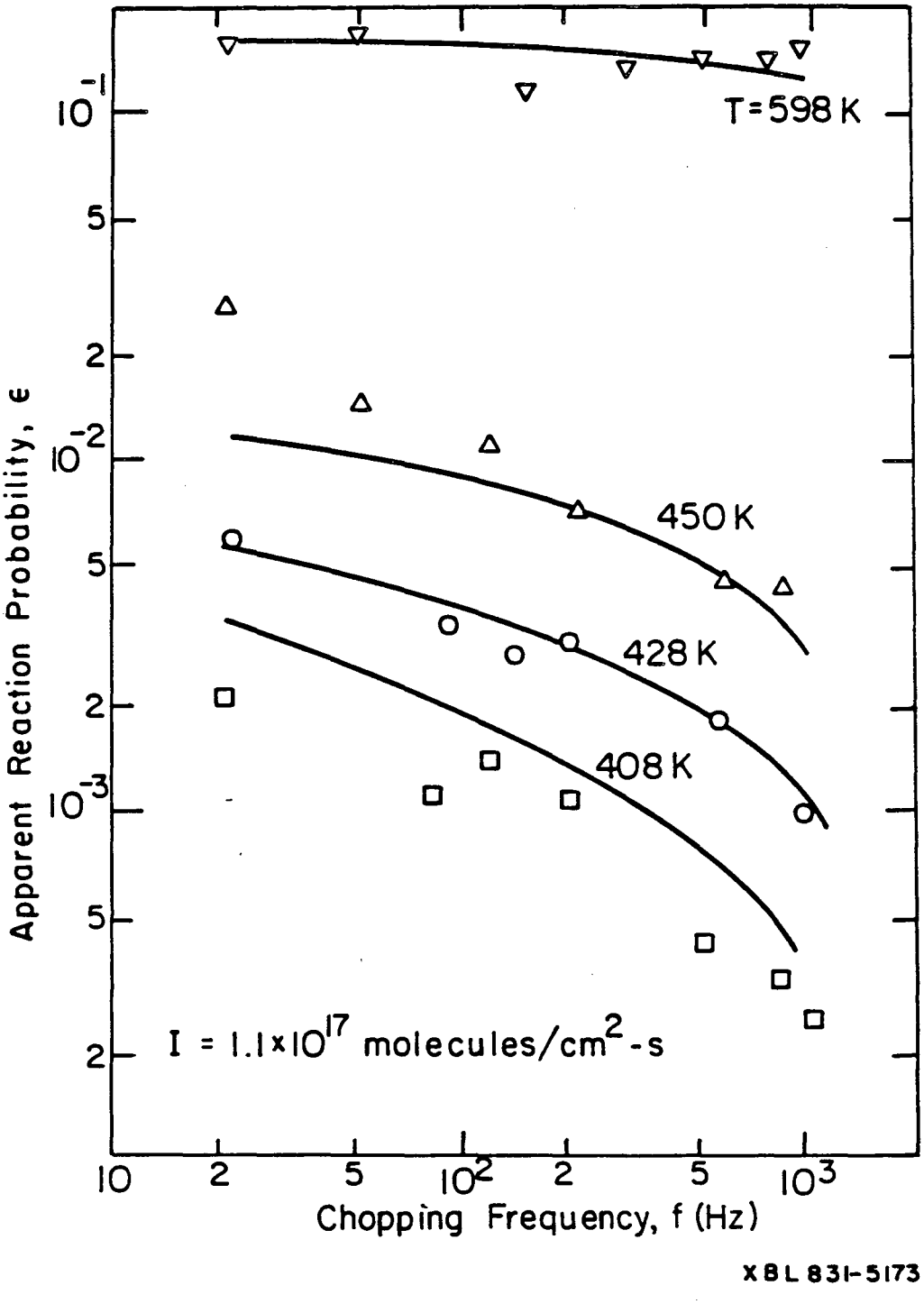
Apparent Reaction Probability, ε
10⁻¹
5
2
10⁻²
5
2
10⁻³
5
2
T=598 K
450 K
428 K
408 K
I = 1.1×10¹⁷ molecules/cm²-s
10
2
5
10²
2
5
10³
Chopping Frequency, f (Hz)
XBL 831-5173

Fig. 6

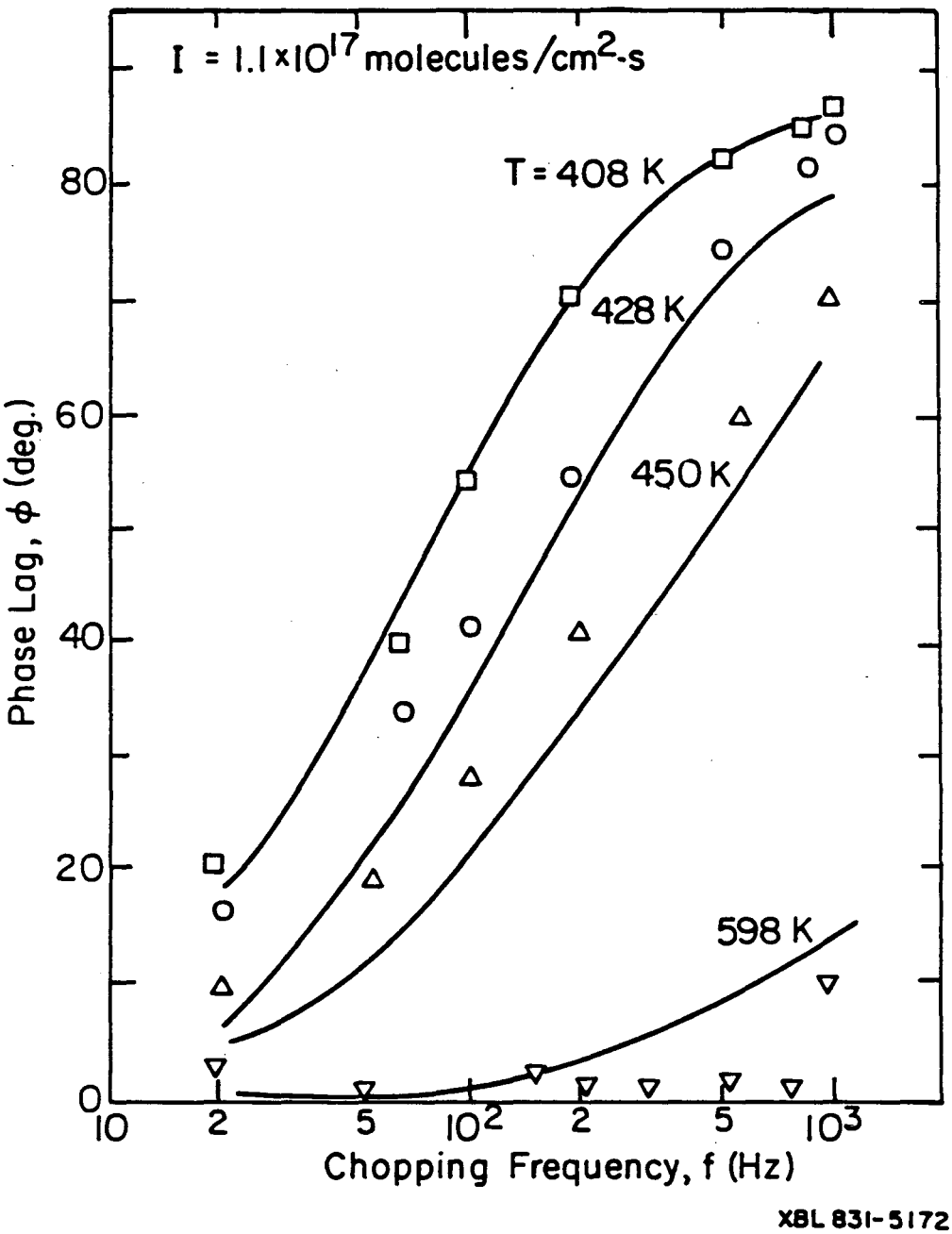
I = 1.1×10^17 molecules/cm^2-s
T = 408 K
428 K
450 K
598 K
Phase Lag, φ (deg.)
0
20
40
60
80
10
2
5
10^2
2
5
10^3
Chopping Frequency, f (Hz)
XBL 831-5172

Fig. 7

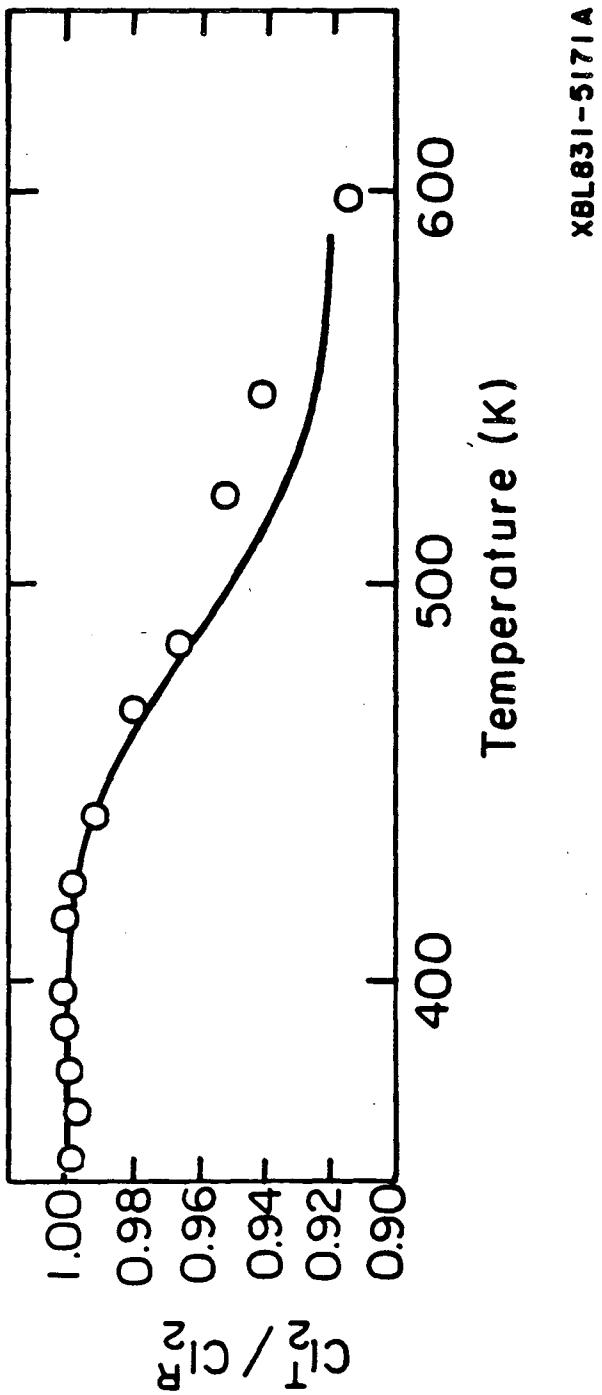
1.00
0.98
0.96
0.94
0.92
0.90
400
500
600
Temperature (K)
Cl_2^T / Cl_2^R
XBL831-5171A

Fig. 8

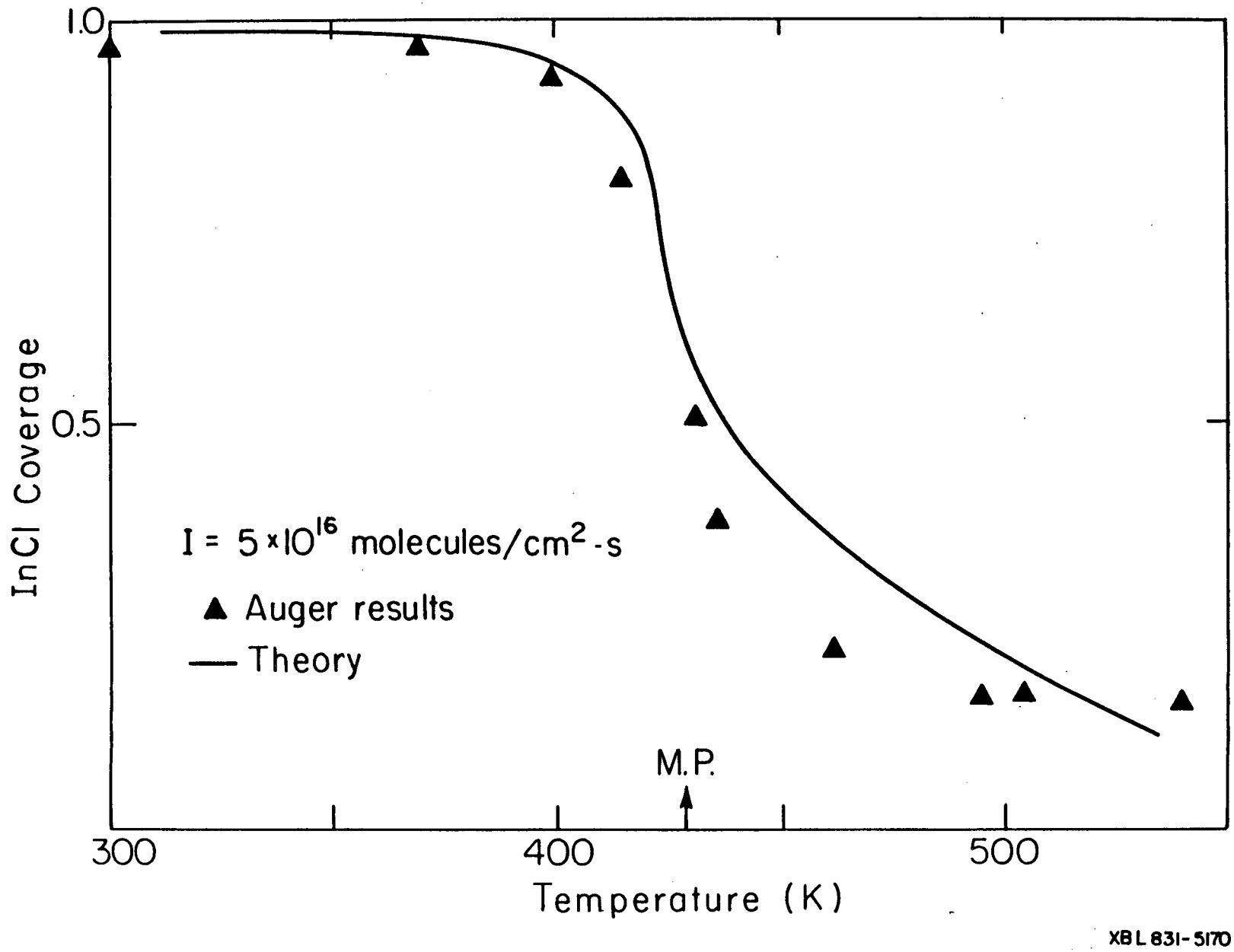
1.0
0.5
InCl Coverage
I = 5 x 10^16 molecules/cm^2 - s
▲ Auger results
— Theory
M.P.
300
400
500
Temperature (K)
XBL 831-5170

Fig. 9

This report was done with support from the Department of Energy. Any conclusions or opinions expressed in this report represent solely those of the author(s) and not necessarily those of The Regents of the University of California, the Lawrence Berkeley Laboratory or the Department of Energy.

Reference to a company or product name does not imply approval or recommendation of the product by the University of California or the U.S. Department of Energy to the exclusion of others that may be suitable.

TECHNICAL INFORMATION DEPARTMENT
LAWRENCE BERKELEY LABORATORY
UNIVERSITY OF CALIFORNIA
BERKELEY, CALIFORNIA 94720